Preprints of the 21st IFAC World Congress (Virtual)
Berlin, Germany, July 12-17, 2020

Adaptive Dual-layer Sliding Mode Control for Wind Turbines with Estimated Wind Speed

Xuguo Jiao, * **Qinmin Yang,** * **Wenchao Meng,** * **Siliang Li,** ** **Yun Shen** **

* *State Key Laboratory of Industrial Control Technology, and the College of Control Science and Engineering, Zhejiang University, Hangzhou, China. (Corresponding Author: qmyang@zju.edu.cn).*
** *Windmagics (Wuhan) Renewable Energy Technology Co., Ltd, Wuhan, China.*

Abstract: Under the circumstance of inaccurate and intermittent wind speed measurement, maximum power capture control of wind turbines is still a hot and challenging topic in wind power generation field. This paper aims at improving wind turbines' power production via an adaptive dual-layer sliding mode controller, with the help of estimated rotor effective wind speed. First, a novel effective wind speed estimation algorithm is proposed based on broad learning system (BLS), the training of which is completed by using data collected from the supervisory control and data acquisition (SCADA) system. Further, the trained BLS can deliver the estimated wind speed in an online manner to determine the optimal generator power command for maximum wind power extraction. In addition, a low-pass filter is designed to smooth the output, which is beneficial for drive train systems' mechanical loads. Thereafter, a sliding mode control theory based maximum power point tracking (MPPT) controller is developed. To compensate for the uncertainties and mitigate the chattering phenomena, dual-layer adaptation laws are designed for the sliding mode controller. Finally, the effectiveness of the proposed control scheme is validated and demonstrated by the FAST (Fatigue, Aerodynamics, Structures, and Turbulence) tool.

Keywords: wind turbines, effective wind speed (EWS) estimation, broad learning system (BLS), maximum power point tracking (MPPT), sliding mode control

1. INTRODUCTION

As one of the most renewable energy resources, wind energy is considered to be an effective solution to tackle with the energy crisis and environmental pollution problems (Soliman et al. (2018)). Global wind power has gained rapid development in the past few decades. According to the World Wind Energy Association (WWEA), the global installed capacity of wind power had grown to 539 GW by the end of 2018 (WWEA (2019)).

Due to the higher wind power capture efficiency and lower operating mechanical loads, variable-speed wind turbines (VSWT) dominate the current market share of wind power generation industry. When VSWT operate in below-rated wind speed region, maximum power point tracking (MPPT) is required to improve the economic benefits of wind farms (Karabacak (2019); Bao et al. (2019)). To achieve this, optimal power reference, which is mainly determined by the effective wind speed (EWS) information, should be provided in the closed MPPT control loop. However, in practice, the measurement of EWS usually suffers from large error or high implementation cost (Jena and Rajendran (2015)). Therefore, how to design an accurate but low-cost EWS estimation approach has become a challenging problem for MPPT control design.

In recent years, many researchers have made their efforts to develop EWS estimation methods (Jena and Rajendran (2015)). In Boukhezzar and Siguerdidjane (2010), Barambones (2019), Song et al. (2017b) and Song et al. (2017a), the authors consider the aerodynamic torque or EWS as an augmented system state, and then use Kalman filter along with the mathematical expression between aerodynamic torque and wind speed or extended Kalman filter to calculate the EWS indirectly or directly. But these model-based methods depend heavily on the system's mathematical model, and thus their field test results are not ideal (Soltani et al. (2013)). To deal with this problem, data-driven EWS estimation methods have become a promising research direction. In Li et al. (2016), authors employ SVR along with genetic algorithm (GA) to build the nonlinear relationship between wind turbines' output data and EWS. But this method needs additional load sensors and thus it will increase the overall implementation cost. Therefore, the data-driven EWS technique needs to be further studied and explored.

Furthermore, to deal with system uncertainties and external disturbances, sliding mode control is widely adopted in the reported MPPT schemes. Integral sliding mode control (ISMC) (Jena and Rajendran (2015)) or third order super twisting sliding mode control (Jena and Rajendran

(2015)) based MPPT controller is designed to compensate the system uncertainties. However, their control signals require the exact information of system parameters. In order to deal with this problem, large enough constant switching gain based sliding mode controller is investigated in Barambones (2019). What's more, sliding mode control with one-layer adaptation switching gain is reported in Beltran et al. (2008) without using the systems' parameters. However, overestimation of the switching gain existing in both Barambones (2019) and Beltran et al. (2008) will affect the control performance and aggravate their chattering effects.

Therefore, in this study, a dual-layer sliding mode MPPT controller is proposed for VSWT, with the help of estimated EWS. First, a model-free EWS estimation approach based on broad learning system (BLS) is proposed. This approach does not need additional load sensors and thus the implementation cost can be reduced. Second, a low-pass filter along with appropriate bandwidth is designed to remove noises from the estimated wind speed and reduce mechanical loads of wind turbines' drive train systems. Moreover, to handle the uncertainties and external disturbances appropriately and mitigate the chattering phenomena in control signal, a sliding mode MPPT controller with dual-layer adaptation laws for the switching gain are developed. Lyapunov theory is employed to guarantee that all signals in the closed-loop system are bounded. Eventually, simulations are conducted to evaluate the performance of the proposed method.

2. DYNAMIC MODEL OF VSWT

This paper considers a common VSWT scheme, as depicted in Fig. 1 (Meng et al. (2013, 2016); Beltran et al. (2008); Moness et al. (2017)). The aerodynamic power captured by the VSWT can be written as

$$P_a = \frac{1}{2}\rho\pi R^2 C_p(\lambda,\beta)v^3 \tag{1}$$

where ρ, R, v, λ and β are respectively the air density, rotor radius, effective wind speed, tip speed ratio and pitch angle. The power coefficient C_p is a nonlinear function of λ and β. Further, the definition of λ can be expressed as

$$\lambda = \frac{R\omega_r}{v} \tag{2}$$

with ω_r being the rotor speed. By utilizing the basic physical laws, the lumped dynamics of the simplified VSWT model can be formulated as

$$\dot{\omega}_r = \frac{1}{J_t}(T_a - K_t\omega_r - T_g) + d(t), \tag{3}$$

where

$$\begin{cases} J_t = \ J_r + n_g^2 J_g \\ K_t = K_r + n_g^2 K_g \\ T_g = \ n_g T_{em} \end{cases} \tag{4}$$

where $d(t)$ represents the external disturbances of VSWT, n_g is the gear box ratio, J_r and J_g are the wind rotor and generator inertias, and K_r and K_g are the external damping constants of rotor and generator, respectively.

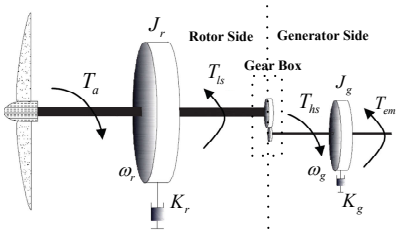

Fig. 1. Two-mass model of the VSWT.

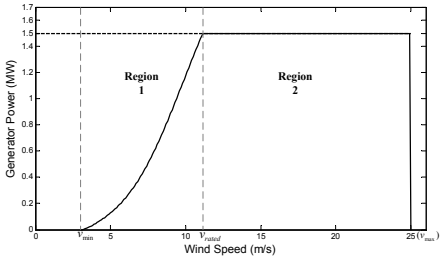

Fig. 2. Operating regions of VSWT.

Further, the generator output power is written as (Meng et al. (2013))

$$P_g = T_g\omega_r. \tag{5}$$

3. CONTROL OBJECTIVE

Fig. 2 shows the static power curve of a VSWT (Meng et al. (2016); Yang et al. (2020)). From Fig. 2, one can conclude that VSWT have two practical operating regions when the wind speed is larger than v_{min} (cut-in wind speed) but lower than v_{max} (cut-off wind speed). In Region 1, to maximize the economic benefits of wind farms, wind turbines are required to achieve MPPT performance by regarding T_g as control signal with β being set as 0^o (Meng et al. (2013, 2016)). Further, the control task of Region 2 is to regulate the generator power at its rated value for the sake of reducing the mechanical loads and guaranteeing the safety of wind turbine systems.

This study focuses on the tracking problem in Region 1. By recalling (1), to obtain MPPT control, P_a should be equal to the following optimal power reference value for each wind speed (Meng et al. (2013); Beltran et al. (2008))

$$P_{amax} = \frac{1}{2}\rho\pi R^2 C_{pmax} v^3 \tag{6}$$

with C_{pmax} being the maximum of C_p. Since the accurate value of v is unavailable in practice, the value of P_{amax} can not be calculated directly. Denoting the estimation of v as $\hat{v}$, the nominal desired generator power can be expressed as

$$P_{ref} = \frac{n_p}{2}\rho\pi R^2 C_{pmax}\hat{v}^3 \tag{7}$$

where $0 < n_p < 1$ is the ratio of power reserve for grid frequency support (Meng et al. (2013)). Further, define the tracking error as

$$e(t) = P_{ref} - P_g. \tag{8}$$

4. EWS ESTIMATION BASED ON BLS

In current wind power industry, there are two ways to measure wind speed for wind turbines, i.e., cup anemometer and LIDAR device. However, the former can only detect the wind speed at one point behind the rotor plane with a large measurement error, which is not a good representation of EWS (Soltani et al. (2013)), and the latter suffers from high implementation cost (Jena and Rajendran (2015)). Therefore, an EWS estimation scheme is expected to achieve the goal of MPPT control in Region 2 of VSWT.

BLS has universal approximation capability and can achieve excellent performance in dealing with regression problems (Chen et al. (2018)). Therefore, in this paper, BLS is employed to build the nonlinear relationship between the selected wind turbines' output variables and the EWS.

Output variables selection is an important step in the EWS estimation of VSWT. In this paper, the following rules are utilized in the wind turbines' output variables selection. First, the selected variables must be obtained directly from the existing supervisory control and data acquisition (SCADA) system so that additional sensors can be eliminated and thus the implementation cost of the EWS estimation method can be reduced. Second, the variables that are insensitive to the control reference but sensitive to the EWS should be included in the set of the selected variables, such that the online estimation performance can be guaranteed. Utilizing the above rules and trial and error methods, the involved output variables for EWS estimation are chosen as: rotor speed ω_r and tower fore-aft deflection d_{fa}, i. e. $X = [\omega_{ri}, d_{fa_i}], i = 1, 2, 3, ..., l_1$ with l_1 being the number of the training samples. The corresponding training targets $Y = [v_i], i = 1, 2, 3, ..., l_1$ are obtained through LIDAR device. After collecting adequate training data for EWS estimation model, the LIDAR can be removed and it is not used in the online implementation phase.

To improve the EWS estimation accuracy, data scaling operation is utilized to scale X to $[0, 1]$. Further, to removed high-frequency components from the estimated EWS and optimize the mechanical loads of the wind turbines, the following low pass filter is utilized

$$G_1(s) = \frac{1}{\tau_1 s + 1}, \tag{9}$$

with $1/\tau_1$ being the bandwidth of (9).

5. CONTROLLER DESIGN

By combining (5) and (8), the dynamics of e can be derived as

$$\dot{e} = -u\omega_r + F \tag{10}$$

where $u = \dot{T}_g$ and the lumped uncertain term $F = \dot{P}_{ref} - T_g\dot{\omega}_r$ is unknown due to the unavailable system parameters, aerodynamics and disturbance. It will be assumed that F and its first time derivative are bounded, i. e., $|F| < F_0$ and $|\dot{F}| < F_1$ with F and F_1 being finite unknown constants.

Moreover, regarding the tracking error $e(t)$ as the sliding variable and employing the sliding mode control theory, the control signal can be represented as (Edwards and Shtessel (2016))

$$u = \frac{1}{\omega_r}((k(t) + \eta)sign(e(t))) \tag{11}$$

with $k(t)$ being a time varying term with adaptation laws which will be explored in the following and $\eta > 0$ is a user defined small constant.

Let $\dot{e}(t) = 0$ and we can obtain the following equivalent control

$$u_{eq} = \frac{F}{\omega_r}. \tag{12}$$

Note that (12) is not the actual control and it is only used for the derivation of the adaptation laws of $k(t)$. The equivalent control u_{eq} can be achieved by low-pass filtering (LPF) the switching term $(k(t) + \eta)sign(e(t))$ in control law (11) (Edwards and Shtessel (2016)). Denoting the estimation of u_{eq} as $\hat{u}_{eq}$, one has

$$\hat{u}_{eq} = \frac{1}{\omega_r}((k(t) + \eta)LPF(sign(e(t)))). \tag{13}$$

In this study, $LPF(\cdot)$ is selected as the following form (Li et al. (2005))

$$G(s) = \frac{1}{\tau s + 1} \tag{14}$$

where $1/\tau$ is the bandwidth. Combining (12) and (13), the lumped uncertain term F can be estimated as

$$\hat{F} = (k(t) + \eta)LPF(sign(e(t))). \tag{15}$$

This study assumes that, for given finite time t_{eq} and τ, there exists $0 < \epsilon_1 < 1$ and $0 < \epsilon_0$ such that

$$||\hat{F}| - |F|| < \epsilon_1|F| + \epsilon_0 \tag{16}$$

holds for $t > t_{eq}$.

To guarantee the sliding motion, the objective will be to ensure (Edwards and Shtessel (2016))

$$k(t) > \frac{1}{\alpha}|\hat{F}(t)| + \epsilon \tag{17}$$

where $0 < \alpha < 1$ and $\epsilon > 0$ are parameters which are chosen according to ϵ_1 and ϵ_0 ensuring

$$\frac{1}{\alpha}|\hat{F}| + \frac{\epsilon}{2} > |F|. \tag{18}$$

Further, a new error variable is designed as

$$\delta(t) = k(t) - \frac{1}{\alpha}|\hat{F}| - \epsilon. \tag{19}$$

It should be noted that if δ=0, then $k(t) = (1/\alpha)|\hat{F}(t)| + \epsilon > |F|$, and this will enforce the sliding motion in (10). Therefore, the problem of maintaining the sliding motion is transformed into making $\delta(t) \to 0$.

Further, the adaptation laws for $k(t)$ with two layers are designed as follows

$$\begin{cases} \dot{k}(t) = -(r_0 + r(t))sign(\delta(t)) \\ \dot{r}(t) = \begin{cases} \gamma|\delta(t)|, & if|\delta(t)| > \delta_0 \\ 0 \quad\quad , & otherwise. \end{cases} \end{cases} \tag{20}$$

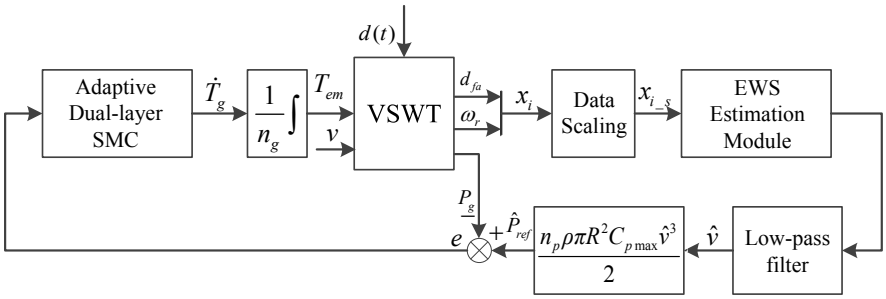

Fig. 3. The proposed MPPT scheme with estimated wind speed.

where $\gamma > 0$ and $\delta_0 > 0$ are user defined constants.

Fig. 3 demonstrates the framework of the proposed MPPT control acheme, and its stability of is analyzed by the Theorem 1.

Theorem 1. Consider the system (10), the control law (11) and the dual layer adaptive mechanism (20). If ϵ is chosen to satisfy

$$\frac{1}{4}\epsilon^2 > \delta_0^2 + \frac{1}{\gamma}(\frac{qF_1}{\alpha})^2, \tag{21}$$

then the proposed control scheme can force $|\delta(t)| < \epsilon/2$ in finite time to obtain a sliding motion. Moreover, $r(t)$, $k(t)$ and $e(t)$ are bounded.

Proof. Please see Appendix A.

6. VERIFICATION STUDIES

To testify the effectiveness of the proposed control strategy, numerical simulations are conducted on FAST (Fatigue, Aerodynamics, Structures, and Turbulence) and Simulink. This software package is developed by NREL (National Renewable Energy Laboratory) and is widely utilized by researchers to validate their wind turbine control algorithms. In this study, the WP 1.5 MW wind turbine model is employed as the testing platform, and its main parameters are demonstrated in Table I (Meng et al. (2013, 2016)).

Table 1. Parameters of the Considered Wind Turbine

R	35 m
n_g	87.965
J_r	$2.962 \times 10^6 \text{kg} \cdot \text{m}^2$
J_g	$53.036\,\text{kg} \cdot \text{m}^2$
ρ	1.225kg/m^3
C_{pmax}	0.5128
λ_{opt}	6.56

Further, control parameters of the proposed scheme are chosen as: $n_p = 0.9$, $r_0 = 100$, $\eta = 5$, $\gamma = 400$, $\alpha = 0.99$, $\epsilon = 4$, $\delta_0 = 300$, $\tau = 0.01$ and $\tau_1 = 2$. In order to analyze the power production improvement performance, the designed MPPT controller is compared with the following standard optimal torque control (OTC) scheme (Li et al. (2016)) which is widely utilized in wind power generation industry (Li et al. (2016))

$$T_{emOTC} = k_{opt}\omega_g^2, (N.m/rpm^2) \tag{22}$$

with $k_{opt} = 0.002585$ designed by NREL (Jonkman and Buhl Jr (2005)). To implement the standard OTC, the term "VSContrl" is set as "1" in the FAST's input file. Further, the proposed method is also compared with the following conventional sliding mode control (CSMS) scheme (Beltran et al. (2008))

$$\dot{T}_g = \frac{(B+c)\frac{e}{|e|+a_0}}{\omega_r}, \quad \dot{B} = |e|\,, \tag{23}$$

where $c = 5$ and $a_0 = 10$ are provided by Meng et al. (2013).

Fig. 4 demonstrates the wind speed estimation performance in the online implementation phase. The RMSE

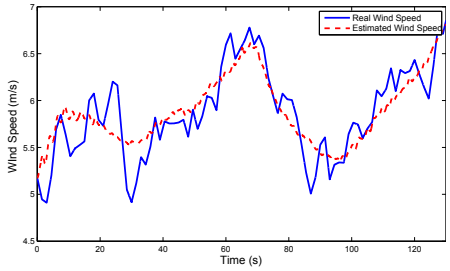

Fig. 4. Online wind speed estimation performance comparison.

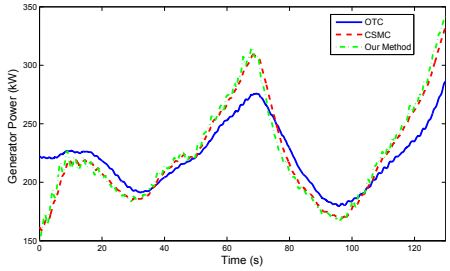

Fig. 5. Generater Power Comparison

.

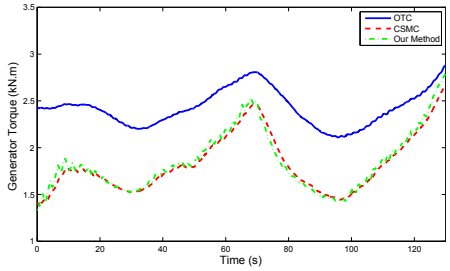

Fig. 6. Rotor Speed Comparison

.

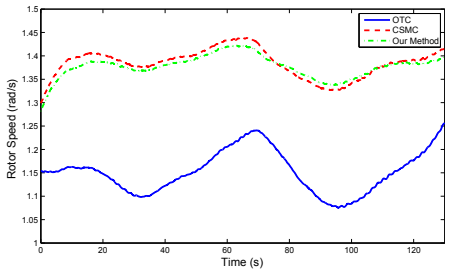

Fig. 7. Generater Torque Comparison.

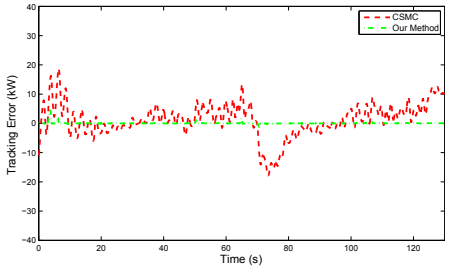

Fig. 8. Tracking Error Comparison.

and MAPE between the real wind speed and estimated wind speed are 0.2352m/s and 3.31%, respectively.

Fig. 5 shows the power outputs of OTC and the proposed controller. Compared with the production generated by OTC and CSMC schemes, the amount of generation of our method with estimated wind speed is respectively increased by 1.12% and 0.51%, which verifies the power production improvement of the proposed scheme. The resulting rotor speeds and generator torques are depicted in Fig. 6 and Fig. 7, respectively. From Fig. 8, we can conclude that our method can achieve better tracking performance than the CSMC approach.

7. CONCLUSION

In this paper, EWS estimation and dual-layer sliding mode control based MPPT scheme of VSWT is investigated. First, a data-driven BLS based EWS estimation approach is proposed, the input of which can be directly obtained from existing SCADA system and thus it will not increase the overall implementation cost. Second, a low-pass filter is designed to smooth the estimated wind speed and thus the mechanical loads in drive train system can be reduced. Furthermore, to ensure the control gain can be large enough to deal with the uncertain unknown dynamics but as small as possible to mitigate chattering effects, a sliding mode MPPT controller along with dual-layer adaptation laws is designed. The rigid stability proof guarantees that all the signals in the closed-loop system are bounded. The verification studies demonstrate the proposed control scheme can achieve more power production than the traditional OTC scheme and CSMC schemes.

ACKNOWLEDGEMENTS

This work is supported by the National Natural Science Foundation of China (61673347, U1609214, 61751205), Key R&D Program of Zhejiang Province (No. 2019C01050), and Key R&D Program of Guangdong Province (No. 2018B010107002).

REFERENCES

Bao, Y., Yang, Q., and Sun, Y. (2019). Iterative modeling of wind turbine power curve based on least-square b-spline approximation. *Asian Journal of Control*.

Barambones, O. (2019). Robust wind speed estimation and control of variable speed wind turbines. *Asian Journal of Control*, 21(2), 856–867.

Beltran, B., Ahmed-Ali, T., and Benbouzid, M.E.H. (2008). Sliding mode power control of variable-speed wind energy conversion systems. *IEEE Transactions on Energy Conversion*, 23(2), 551–558.

Boukhezzar, B. and Siguerdidjane, H. (2010). Nonlinear control of a variable-speed wind turbine using a two-mass model. *IEEE Transactions on Energy Conversion*, 26(1), 149–162.

Chen, C.P., Liu, Z., and Feng, S. (2018). Universal approximation capability of broad learning system and its structural variations. *IEEE Transactions on Neural Networks and Learning Systems*, 30(4), 1191–1204.

Edwards, C. and Shtessel, Y.B. (2016). Adaptive continuous higher order sliding mode control. *Automatica*, 65, 183–190.

Jena, D. and Rajendran, S. (2015). A review of estimation of effective wind speed based control of wind turbines. *Renewable and Sustainable Energy Reviews*, 43, 1046–1062.

Jonkman, J.M. and Buhl Jr, M.L. (2005). FAST user's guide-updated august 2005. Technical report, National Renewable Energy Lab.(NREL), Golden, CO (United States).

Karabacak, M. (2019). A new perturb and observe based higher order sliding mode MPPT control of wind turbines eliminating the rotor inertial effect. *Renewable Energy*, 133, 807–827.

Li, D.Y., Cai, W.C., Li, P., Jia, Z.J., Chen, H.J., and Song, Y.D. (2016). Neuroadaptive variable speed control of wind turbine with wind speed estimation. *IEEE Transactions on Industrial Electronics*, 63(12), 7754–7764.

Li, H., Shi, K., and McLaren, P. (2005). Neural-network-based sensorless maximum wind energy capture with compensated power coefficient. *IEEE Transactions on Industry Applications*, 41(6), 1548–1556.

Meng, W., Yang, Q., and Sun, Y. (2016). Guaranteed performance control of dfig variable-speed wind turbines. *IEEE Transactions on Control Systems Technology*, 24(6), 2215–2223.

Meng, W., Yang, Q., Ying, Y., Sun, Y., Yang, Z., and Sun, Y. (2013). Adaptive power capture control of variable-speed wind energy conversion systems with guaranteed transient and steady-state performance. *IEEE Transactions on Energy Conversion*, 28(3), 716–725.

Moness, M., Mahmoud, M.O., and Moustafa, A.M. (2017). A real-time heterogeneous emulator of a high-fidelity utility-scale variable-speed variable-pitch wind turbine. *IEEE Transactions on Industrial Informatics*, 14(2), 437–447.

Soliman, M.A., Hasanien, H., Azazi, H.Z., El-Kholy, E., and Mahmoud, S.A. (2018). An adaptive fuzzy logic control strategy for performance enhancement of a grid-connected pmsg-based wind turbine. *IEEE Transactions on Industrial Informatics*.

Soltani, M.N., Knudsen, T., Svenstrup, M., Wisniewski, R., Brath, P., Ortega, R., and Johnson, K. (2013). Estimation of rotor effective wind speed: A comparison. *IEEE Transactions on Control Systems Technology*, 21(4), 1155–1167.

Song, D., Yang, J., Cai, Z., Dong, M., Su, M., and Wang, Y. (2017a). Wind estimation with a non-standard extended Kalman filter and its application on maximum power extraction for variable speed wind turbines. *Applied Energy*, 190, 670–685.

Song, D., Yang, J., Dong, M., and Joo, Y.H. (2017b). Kalman filter-based wind speed estimation for wind turbine control. *International Journal of Control, Automation and Systems*, 15(3), 1089–1096.

WWEA (2019). Wind power capacity worldwide reaches 597 GW, 50.1 GW added in 2018. 2019. [Online]. Available: https://wwindea.org/blog/2019/02/25/wind-power-capacity-worldwide-reaches-600-gw-539-gw-added-in-2018/. Accessed on: Sep. 22, 2019.

Yang, Q., Jiao, X., Luo, Q., Chen, Q., and Sun, Y. (2020). L1 adaptive pitch angle controller of wind energy conversion systems. *ISA transactions*.

Appendix A. PROOF OF THEOREM 1

Proof. First, define

$$e_1(t) = q\frac{F_1}{\alpha} - r(t) \tag{A.1}$$

with $q > 1$ being a safety margin chosen to ensure $(d|\hat{F}(t)|/dt) < qF_1$.

Recalling (19), (20) and (A.1), the dynamics of $\delta(t)$ and $e_1(t)$ can be derived as

$$\begin{cases} \dot{\delta}(t) = -(r_0 + \dfrac{qF_1}{\alpha} - e_1(t))sign(\delta(t)) + \dfrac{1}{\alpha}\dfrac{d|\hat{F}(t)|}{dt} \\ \dot{e}_1(t) = \begin{cases} -\gamma|\delta(t)|, \ if \ |\delta(t)| > \delta_0 \\ 0 \qquad\quad , \ otherwise. \end{cases} \end{cases} \tag{A.2}$$

Further, consider the following Lyapunov function

$$V = \frac{1}{2}\delta^2 + \frac{1}{2\gamma}e_1^2. \tag{A.3}$$

Taking its time derivative and utilizing (A.2), one has

$$\begin{aligned} \dot{V} &= \delta\dot{\delta} + \frac{1}{\gamma}e_1\dot{e}_1 \\ &\le -r_0\left|\delta(t)\right| + (e_1(t) - \frac{qF_1}{\alpha})\left|\delta(t)\right| + |\delta(t)|\frac{qF_1}{\alpha} \\ &+\frac{1}{\gamma}e_1\dot{e}_1 \\ &= -r_0\left|\delta(t)\right| + e_1(t)\left|\delta(t)\right| + \frac{1}{\gamma}e_1\dot{e}_1. \end{aligned} \tag{A.4}$$

Suppose $r(0) = 0$, then $r(t) > 0$ according to (20). Therefore, it can be concluded that $e_1(t) < (qF_1)/\alpha$ for all time.

If $|\delta(t)| > \delta_0$, one has

$$\dot{V} \le -r_0|\delta(t)| \tag{A.5}$$

If $|\delta(t)| \le \delta_0$ and $e_1(t) < 0$, (A.5) also holds.

Moreover, consider the following rectangle

$$\Re = \{(\delta, e_1) : |\delta| \le \delta_0, 0 \le e_1 \le \frac{qF_1}{\alpha}\}. \tag{A.6}$$

It can be concluded that $\dot{V} \le -r_0|\delta(t)|$ outside the rectangle $\Re$. To enclose $\Re$, the smallest ellipse centered at the origin is chosen as

$$\vartheta = \{(\delta, e_1) : V(\delta, e_1) \le \bar{r}\} \tag{A.7}$$

where

$$\bar{r} = \frac{1}{2}\delta_0^2 + \frac{1}{2\gamma}(\frac{qF_1}{\alpha})^2. \tag{A.8}$$

Obviously, ϑ is an invariant set, i. e., once the trajectory $(\delta(t), e_1)$ as the solution of V, enters ϑ, it cannot leave ϑ. Therefore, from (21), $\delta(t) < \epsilon/2$ holds.

Further, when $(\delta(t), e_1)$ does not enter ϑ, according to the above conclusion $\dot{V} \le -r_0|\delta(t)|$ outside ϑ, we have

$$\int_0^\infty r_0|\delta(t)| \le V(0). \tag{A.9}$$

Since $(\delta(t), e_1)$ is bounded, from (A.2) $\dot{\delta}(t)$ is also bounded. Thus, $\delta(t)$ and hence $|\delta(t)|$ are uniformly continuous. Recalling (A.9) and according to Barbalat's Lemma, we can conclude that $|\delta(t)| \to 0$ as $t \to \infty$. Consequently, there exists a finite time t_0 such that

$$|\delta(t)| < \frac{\epsilon}{2}, t > t_0 \tag{A.10}$$

Therefore, one can conclude that $|\delta(t)| < \frac{\epsilon}{2}$ in finite time for whether $(\delta(t), e_1)$ enters ϑ or not.

Moreover, recalling (19) yields

$$|\delta(t)| = |k(t) - \frac{1}{\alpha}|\hat{F}(t)| - \epsilon| < \frac{\epsilon}{2}. \tag{A.11}$$

Thus, we have

$$k(t) > \frac{1}{\alpha}|\hat{F}(t)| + \frac{\epsilon}{2} > |F(t)|. \tag{A.12}$$

Then, it concludes that the sliding motion on $e = 0$ can be maintained. Since $\delta(t)$ and $e_1(t)$ are bounded, combining(16), (19) and (A.1), one has

$$\begin{cases} r(t) < \dfrac{qF_1}{\alpha} + |e_1(t)| \\ k(t) < |\delta(t)| + (1+\epsilon_1)\dfrac{F_0}{\alpha} + \dfrac{\epsilon_0}{\alpha} + \epsilon \end{cases} \tag{A.13}$$

Therefore, $r(t)$ and $k(t)$ are bounded.

Furthermore, consider another Lyapunov function

$$V_1 = \frac{1}{2}e^2. \tag{A.14}$$

By recalling (10), (11) and (A.12), the derivative of V_1 can be written as

$$\begin{aligned} \dot{V}_1 &= e\dot{e} \\ &\le -\eta|e| - k(t)|e| + F(t)|e|\,. \\ &\le -\eta|e| \end{aligned} \tag{A.15}$$

Therefore, $e(t)$ is also bounded according to the Lyapunov stability theory.